

# Probing molecular frame photoionization via laser generated high-order harmonics from aligned molecules

Anh-Thu Le,<sup>1</sup> R. R. Lucchese,<sup>2</sup> M. T. Lee,<sup>3</sup> and C. D. Lin<sup>1</sup>

<sup>1</sup>*Department of Physics, Cardwell Hall, Kansas State University, Manhattan, KS 66506, USA*

<sup>2</sup>*Department of Chemistry, Texas A&M University, College Station, Texas 77843-3255, USA*

<sup>3</sup>*Departamento de Química, Universidade Federal de São Carlos, 13565-905, São Paulo, Brazil*

(Dated: November 3, 2018)

Present photoionization experiments cannot measure molecular frame photoelectron angular distributions (MFPAD) from the outermost valence electrons of molecules. We show that details of the MFPAD can be retrieved with high-order harmonics generated by infrared lasers from aligned molecules. Using accurately calculated photoionization transition dipole moments for fixed-in-space molecules, we show that the dependence of the magnitude and phase of the high-order harmonics on the alignment angle of the molecules observed in recent experiments can be quantitatively reproduced. This result provides the needed theoretical basis for ultrafast dynamic chemical imaging using infrared laser pulses.

PACS numbers: 33.80.Eh, 42.65.Ky

Photoionization (PI) is the basic process that allows the most direct investigation of molecular structure. Measurements of total, partial and differential PI cross sections have a long history. Until recently, however, almost all the experiments are performed from an ensemble of randomly oriented molecules. Thus the rich dynamical structure of photoelectron angular distribution for fixed-in-space molecules predicted in the seminal paper by Dill [1] more than 30 years ago still remains largely unexplored. In recent years, fixed-in-space PI has been investigated with x-ray or VUV photons by using the photoelectron-photoion coincidence technique [2, 3]. Following inner-shell or inner-valence-shell ionization the molecular ion dissociates. The molecular axis at the time of ionization is inferred from the direction of motion of the fragment ion if the dissociation time is short compared to the rotational period. Clearly this method is not applicable to PI from the highest occupied molecular orbital (HOMO).

Consider photoionization of a linear molecule. For a polarized light, the differential cross section can be expressed in the general form [4] (atomic units are used throughout, unless otherwise indicated)

$$\frac{d^2\sigma}{d\Omega_{\mathbf{k}}d\Omega_{\mathbf{n}}} = \frac{2(2\pi)^3 E}{3c} \left| \sum_{lm\mu} I_{lm\mu} Y_{lm}^*(\Omega_{\mathbf{k}}) Y_{1\mu}^*(\Omega_{\mathbf{n}}) \right|^2. \quad (1)$$

In this expression, the molecular axis is fixed, the directions of light polarization and electron emission are given by  $\Omega_{\mathbf{n}}$  and  $\Omega_{\mathbf{k}}$ , respectively. This is called the molecular frame photoionization angular distribution (MFPAD). We calculate the continuum wavefunction  $\Psi_{f,klm}^-$  and the dipole  $I_{lm\mu} = k^{1/2} \langle \Psi_i | r_{\mu} | \Psi_{f,klm}^- \rangle$  (with  $r_{\mu} = z$  for linear polarization) using the iterative Schwinger variational method [4] within the complete-active-space configuration interaction scheme [5]. To compare with measurements, integration of Eq. (1) over unobserved variables

has to be performed, thus losing much valuable information on the structure of the molecule.

In this Letter we show that recent advances in the generation of high-order harmonics from molecules by intense infrared lasers has made it possible to probe fixed-in-space molecular PI from HOMO. Gas phase molecules can be impulsively aligned by a short sub-picosecond infrared laser [6]. After the pulse is turned off, molecules will be partially aligned or anti-aligned at the time intervals of rotational revival [7, 8]. During these revivals which last for tens or hundreds of femtoseconds, another probe pulse can be used to illuminate molecules to observe the emission of high-order harmonics. The first experiment of this type was reported by Kanai *et al.* [8] using N<sub>2</sub>, O<sub>2</sub> and CO<sub>2</sub> molecules. Since then many more experiments have been reported [7, 9, 10, 11, 12, 13]. To study the dependence of high-order harmonics generation (HHG) on the alignment of molecules, the probe laser can be applied at the different time as the molecules evolve, or by changing the direction of the probe laser polarization at a fixed time delay. More recently, HHG from mixed gases [10, 11] and interferometry technique [12] have also been used such that the phase of the HHG can also be measured.

HHG is a highly nonlinear process and can be understood using the three-step model [14]. Electrons are first released from the molecule by tunnel ionization and thrown into the laser field. As the laser's electric field changes direction, the electrons may be driven back to the ion core after gaining kinetic energy from the field. When the electrons recombine with the ion, high-order harmonic photons are emitted. Since the photo-recombination (PR) in the last step is the time-reversed process of PI, it is thus expected that HHG spectra hold valuable information on the molecule. Indeed, HHG spectra had been used to extract the HOMO in N<sub>2</sub> using tomographic method [15]. However the tomographic

method relies exclusively on approximating the continuum electrons by plane waves which is known to fail in general from the PI studies. In [16, 17] we have developed a quantitative rescattering theory (QRS) for HHG where complex HHG dipole moment  $D(\omega, \theta)$  from a fixed-in-space molecule can be expressed as a product of the transition dipole  $d(\omega, \theta) = \sum_{lm\mu} I_{lm\mu} Y_{lm}^*(\Omega_{\mathbf{k}}) Y_{1\mu}^*(\Omega_{\mathbf{n}})$  (with  $\mathbf{k} \parallel \mathbf{n}$ ) and the returning electron wave-packet  $W(E_k, \theta)$ ,

$$D(\omega, \theta) = W(E_k, \theta) \times d(\omega, \theta). \quad (2)$$

This model establishes the relation between the induced dipole moment with the transition dipole for PR (or PI). Here  $\theta$  is the alignment angle of the molecular axis with respect to the polarization direction of the probe laser, and  $\omega = I_p + E_k$ , with  $\omega$  the photon energy of the harmonics,  $I_p$  the ionization potential, and  $E_k = k^2/2$  the “incident” energy of the returning electron. The validity of this equation has been established for atomic targets (no  $\theta$  dependence for atoms) [16, 17] as well as for  $\text{H}_2^+$  target [18]. In both cases, HHG spectra can be calculated accurately by solving the time-dependent Schrödinger equation (TDSE). In this Letter, we obtained transition dipole  $d(\omega, \theta)$  from the state-of-the-art PI calculations. The wave-packet  $W(E_k, \theta)$  is obtained from the strong-field approximation (SFA)[16, 18, 19]. We then use Eq. (2) to obtain  $D(\omega, \theta)$  for each fixed-in-space molecule. To compare with experiments, proper coherent convolution with the partial alignment of molecules has to be carried out [see Eq. (2) of Ref. [10]].

In Fig. 1(a), we show the theoretical  $\text{CO}_2$  PI differential cross section for the emission direction along the light polarization ( $\mathbf{k} \parallel \mathbf{n}$ ), which are to be compared to HHG data below. By changing the orientation of the fixed-in-space molecule, complementary information on the angular distribution of photoelectrons from fixed-in-space molecules is obtained. In order to compare with HHG data, the photon energies are expressed in units of photon energy of 800-nm laser (1.55 eV). First, we note that the differential cross section is large when the molecule is aligned at a large angle. The cross sections vanish at  $\theta = 0$  and  $\pi/2$  due to the  $\pi_g$  symmetry of the HOMO and the dipole selection rule for the final state. Second, the cross section shows near-zero minima for angles around  $35^\circ$  to  $45^\circ$  for harmonics above the 25th order, or H25. The position of the minimum moves to a larger angle, as energy increases. These minima have been interpreted as evidence of interference of electron waves from the atomic centers. In Fig. 1(b), we show the phase of the PI dipole vs photon energy, for alignment angles from  $20^\circ$  to  $60^\circ$ . Between  $30^\circ$  and  $45^\circ$  the dipole phase undergoes rapid change between H25 and H39. This is the region where the cross sections are near the minima [see Fig. 1(a)]. The phase change is about 2.0 to 2.5, instead of  $\pi$  as should be expected if the cross section indeed goes to zero. For angles below  $20^\circ$  and above  $60^\circ$  the phase evolves smoothly vs photon energy. The “rich” structures in the theoret-

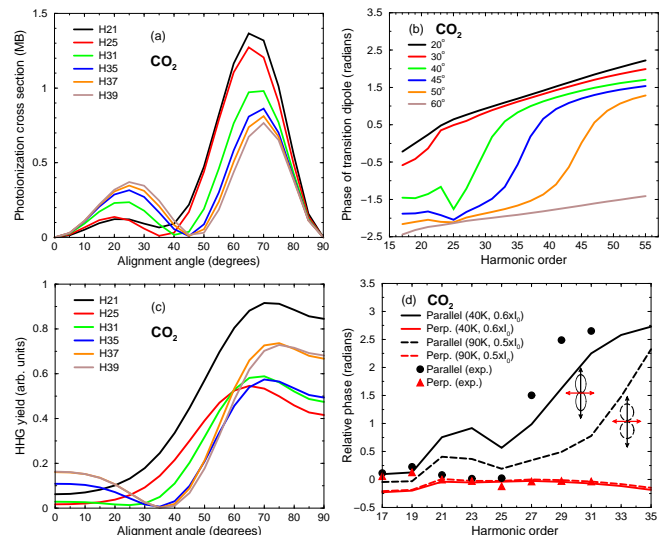


FIG. 1: (Color online)  $\text{CO}_2$  differential photoionization cross section (a) and phase of the transition dipole (b). The photon energies are expressed in units of harmonic orders for 800-nm laser. (c) HHG yield as function of angle between pump and probe laser polarization directions. The laser intensity and duration are of  $0.55 \times I_0$  ( $I_0 = 10^{14} \text{ W/cm}^2$ ), and 120 fs for the pump pulse, and  $2.5 \times I_0$  and 25 fs for the probe pulse. Rotational temperature is taken to be 105 K. (d) Harmonic phase (relative to the phase from Kr) for parallel aligned and perpendicular aligned ensembles, under two sets of parameters (solid and dashed lines) that lead to two different degrees of alignment distributions. Experimental data from Boutu *et al.* [13] are shown as symbols.

cal amplitude and phase of  $d(\omega, \theta)$  shown in Fig. 1 have never been observed directly in PI experiments. Below we show that they have been observed in recent HHG measurements.

In Fig. 1(c) we show the simulated typical HHG yields from aligned  $\text{CO}_2$ , as a function of the angle between the pump and probe lasers polarization directions. These results are consistent with recent experiments [13, 20, 21], and with earlier theoretical results [22, 23, 24]. The results also resemble the data for the induced dipole retrieved from mixed gases experiments by Wagner *et al.* [10] (see their Fig. 4). In our simulation, the laser parameters are taken from the experiment of [12]. The alignment distribution is obtained from numerical solution of the TDSE within the rotor model [6, 22, 23]. At the delay time corresponding to the maximum alignment near half-revival (1/2 of the rotational period), a probe beam with polarization direction varying from 0 to  $90^\circ$  is used to generate high-order harmonics. Comparing Fig. 1(c) with Fig. 1(a), we note that the HHG yields follow the general angular and photon energy dependence of the the differential PI cross sections. Both figures show large yields at large angles, and minima near  $35^\circ$  for harmonic orders above H31. Due to the averaging over the molecular alignment distributions, the angular dependence of

HHG is smoother.

We next show that the phase of fixed-in-space PI transition dipole can also be probed by comparing to the phase of the harmonics. Experimentally the harmonics phase can be extracted from measurements of HHG using mixed gases [11, 13] or interferometry method [12]. In Fig. 1(d), we show the recent experimental data of Boutu *et al.* [13] where the harmonics phases (relative to that from Kr) are obtained for the parallel aligned and perpendicularly aligned ensembles, shown by black and red symbols, respectively. For the latter, the phase does not change much within H17 to H31. For the parallel aligned molecules, the phase jump from H17 to H31 was reported to be  $2.0 \pm 0.6$  radians (in the figure it was shown at 2.6 radians). Our simulation results are shown for two different ensembles, with alignment distributions confined in a cone angle of  $25^\circ$  and  $35^\circ$  at half maximum, resulting from different pump beams and gas temperatures (see Caption). From Fig. 1(b), we note that for a fixed harmonic, the phase from the parallel aligned ensemble is larger if the angular spread of the molecular distributions is smaller. Therefore, the position of the phase jump for the less aligned ensemble (dashed line) slightly shifted toward higher energies. For the perpendicularly aligned molecules, the phase is small and does not change much with the harmonic order. This is consistent with the phase shown in Fig. 1(b). Thus the phase of HHG in Fig. 1(d) is seen to mimic the phase of the PI dipole shown in Fig. 1(b).

Next we show in Fig. 2 how the HHG yields change with the time delay near the 3/4-revival where the molecule can be most strongly aligned. Our simulations were carried out with the laser parameters from Zhou *et al.* [12]. The degree of alignment (top panel), as measured by  $\langle \cos^2 \theta \rangle$  is maximum when molecules are maximally aligned (vertically in the figure) and minimum when molecules are anti-aligned. Our results are shown for the same harmonics that had been analyzed in [12] (see their Fig. 2 - according to a new assignment by the authors of [12], the harmonic orders should be properly shifted down by two orders, compared to the ones given in their original paper [21]). For the lower harmonics H21 and H25, the yields follow the inverse of the alignment parameter. This is easily understood from Fig. 1(a) which shows that the PI cross sections at large angles are much larger than at small angles. For the higher orders, Fig. 1(a) indicates that the PI cross sections show two humps, with the one at smaller angles only a factor of about two to three times smaller than the other. Qualitatively, this explains why the HHG yields for H31 and up show a pronounced peak for the parallel alignment. We note a quantitatively good agreement between our calculations and the experimental data.

Evolution of the HHG yields has also been studied by Wagner *et al.* [10] using the mixed gases technique. The yield and phase for H31 vs time delay near half-revival

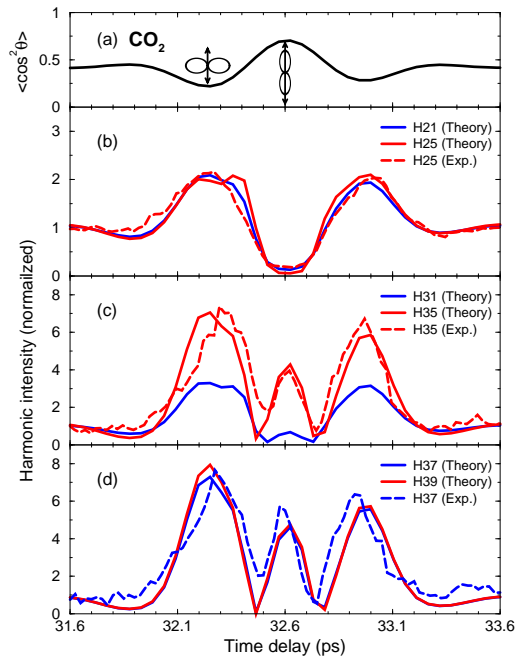


FIG. 2: (Color online) Normalized HHG yield (vs isotropically distributed molecules) from  $\text{CO}_2$  for different harmonics as function of pump-probe delay time near 3/4-revival. Laser parameters are the same as in Fig. 1(c). The experimental data are taken from Zhou *et al.* [12]. The alignment parameter  $\langle \cos^2 \theta \rangle$  is plotted for reference (a).

are shown in Fig. 3(c) and (b), respectively. Our simulations (solid lines) are also in good agreement with these measurements. The HHG yield is small when the molecules are maximally aligned. This is in agreement with H31 seen in Fig. 2(c) for the delay time near 3/4-revival. However, we note that the phase is maximum when the molecules are maximally aligned. This can be understood from the phase in Fig. 1(b) where it shows that the phase is large when the alignment angle is small. It also shows that the phase is small when the alignment angle is large, thus for anti-aligned molecules the phase of the HHG should be small, as seen in the experimental data and in the simulation.

We remark that the laser intensity used in the JILA experiments is quite high, thus the effect of the depletion of the ground state by the laser should be considered [22, 23, 25]. For  $\text{CO}_2$ , the alignment dependence of the ionization rate is still not fully settled yet. The results from the MO-ADK theory [26], the SFA theory and the experiment [27] all disagree with each other, with the SFA predicting a peak near  $40^\circ$ , compared to  $30^\circ$  from MO-ADK theory, and  $45^\circ$  from experiment [27]. Using ionization rates from MO-ADK, we have not been able to simulate experimental data accurately. We thus used ionization rates from SFA, except that we renormalize the SFA rate to that of the MO-ADK rate at laser intensity of  $I_0$ , which gives a factor of 10. Note that the same

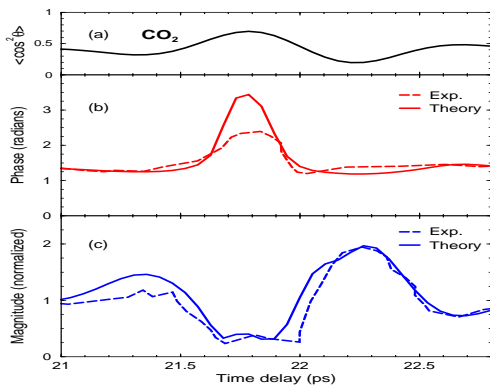


FIG. 3: (Color online) Alignment parameter  $\langle \cos^2 \theta \rangle$  (a), phase (b) and magnitude (c) of the 31th order harmonic from  $\text{CO}_2$ , as functions of pump-probe delay time near half-revival. The experimental data are taken from Wagner *et al* [10]. The laser intensity and duration are of  $0.38 \times I_0$  and 140 fs for the pump, and  $2.5 \times I_0$  and 30 fs for the probe. Rotational temperature is taken to be 70 K.

correction factor has been found for the SFA ionization from Kr, which has almost the same ionization potential as for  $\text{CO}_2$ . With the corrected SFA rate, we found that our simulations give a better quantitative agreement with the JILA data [12].

We have also studied  $\text{N}_2$  molecules. The fixed-in-space differential PI cross sections are shown in Fig. 4(a). For H17 to H21 the cross sections are quite large since this is in the tail region of the famous shape resonance in  $\text{N}_2$ . For these orders, the cross sections are highly forwardly peaked. For energies above H25, the cross sections become much smaller, and they are of the same order of magnitude between parallel and perpendicular alignments. However, note that the cross sections have minima at large angles around  $60^\circ - 70^\circ$ . The (normalized) HHG spectra of  $\text{N}_2$  has been measured vs the time delay in [7]. Their results are shown in Fig. 4(c), along with the results from our simulation. Clearly for H21-H25, the yield (normalized to the isotropic distribution case) is much larger than that from the higher harmonics when the molecules are maximally aligned, which is consistent with the PI cross sections shown in Fig. 4(a). Once again, the experimental HHG spectra can be reproduced within the QRS based on the accurate dipole transition amplitudes from PI calculation, thus allowing us to probe the MFPAD for HOMO.

In conclusions, we have shown that molecular frame photoionization can be probed directly using laser-generated high-order harmonics from aligned molecules. This method is particularly useful for probing fixed-in-space molecular photoionization from the HOMOs. Alternatively, using accurate PI dipole matrix elements calculated from the state-of-the-art molecular photoionization codes, we have illustrated that the nonlinear HHG spectra can be accurately calculated [see Eq. (2)]. By

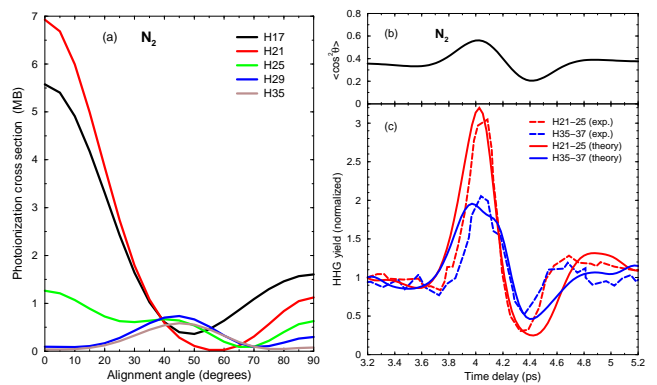


FIG. 4: (Color online) (a) Same as in Fig. 1(a), but for  $\text{N}_2$ . (b) and (c): Alignment parameter  $\langle \cos^2 \theta \rangle$  and harmonic yields H21-H25 and H35-H37 from  $\text{N}_2$ . The experimental data and laser parameters are taken from Itatani *et al* [7].

varying laser intensity, HHG spectra from lower-lying orbitals can also be similarly probed [28]. Having established the connection between HHG and the PI dipole matrix elements, see Eq. (2), time-resolved PI cross sections can be extracted from HHG spectra in a typical pump-probe experimental setup, thus opening up the opportunity of using infrared laser pulses for ultrafast dynamic chemical imaging.

We thank X. Zhou, N. Wagner, M. Murnane, H. Kapteyn, and P. Salieres for communicating their results to us and the valuable discussions. This work was supported in part by the Chemical Sciences, Geosciences and Biosciences Division, Office of Basic Energy Sciences, Office of Science, U. S. Department of Energy.

- 
- [1] D. Dill, J. Chem. Phys. **65**, 1130 (1976).
  - [2] T. Weber *et al.*, Nature (London) **431**, 437 (2004).
  - [3] X.-J. Liu *et al.*, Phys. Rev. Lett. **101**, 023001 (2008).
  - [4] R. R. Lucchese *et al.*, Phys. Rev. A **25**, 2572 (1982).
  - [5] R. E. Stratmann and R. R. Lucchese, J. Chem. Phys. **102**, 8494 (1995).
  - [6] H. Stapelfeldt and T. Seideman, Rev. Mod. Phys. **75**, 543 (2003).
  - [7] J. Itatani *et al.*, Phys. Rev. Lett. **94**, 123902 (2005).
  - [8] T. Kanai *et al.*, Nature **435**, 470 (2005).
  - [9] C. Vozzi *et al.*, Phys. Rev. Lett. **95**, 153902 (2005).
  - [10] N. Wagner *et al.*, Phys. Rev. A **76**, 061403 (2007).
  - [11] T. Kanai *et al.*, Phys. Rev. A **77**, 041402 (2008).
  - [12] X. Zhou *et al.*, Phys. Rev. Lett. **100**, 073902 (2008).
  - [13] W. Boutou *et al.*, Nature Physics **4**, 545 (2008).
  - [14] P. B. Corkum, Phys. Rev. Lett. **71**, 1994 (1993).
  - [15] J. Itatani *et al.*, Nature **432**, 867 (2004).
  - [16] A. T. Le *et al.*, Phys. Rev. A **78**, 023814 (2008).
  - [17] T. Morishita *et al.*, Phys. Rev. Lett. **100**, 013903 (2008).
  - [18] A. T. Le *et al.*, J. Phys. B **41** 081002 (2008).
  - [19] M. Lewenstein *et al.*, Phys. Rev. A **49**, 2117 (1994).
  - [20] Y. Mairesse *et al.*, J. Mod. Optics **55**, 2591 (2008).

- [21] X. Zhou and M. Murnane, private communication.
- [22] A. T. Le *et al.*, Phys. Rev. A **73**, 041402(R) (2006).
- [23] A. T. Le *et al.*, J. Mod. Optics **54**, 967 ( 2007).
- [24] R. de Nalda *et al.*, Phys. Rev. A **69**, 031804(R) (2004).
- [25] P. Liu *et al.*, Phys. Rev. A **78**, 015802 (2008).
- [26] X. M. Tong *et al.*, Phys. Rev. A **66**, 033402 (2002).
- [27] D. Pavicic *et al.*, Phys. Rev. Lett. **98**, 243001 (2007).
- [28] B. K. McFarland *et al.*, Science **322**, 1232 (2008).